

The Energy Flow of X-Rays in Germanium Single Crystals

L. Gerward

Laboratory of Applied Physics III, Technical University of Denmark, Lyngby, Denmark

(Z. Naturforsch. **28 a**, 577—580 [1973] ; received 19 January 1973)

Dedicated to Gerhard Borrmann on the occasion of his 65th birthday

The energy flow of the X-ray wave fields set up by diffraction in a germanium single crystal has been studied by shadow sharpness measurements. The shadow has been produced by an absorbing wire close to the X-ray entrance surface of the crystal. Intensity profiles have been observed in the wavelength range from 1.541 Å to 0.709 Å, including the K absorption edge of germanium at 1.117 Å. It is shown that the angular divergence of the energy flow is almost independent of the wavelength on each side of the absorption edge. The angular divergence is considerably reduced when passing the absorption edge from the low-energy side to the high-energy side, the thickness of the crystal being kept constant.

1. Introduction

The dynamical theory of diffraction in a perfect lattice predicts that a number of wave fields are produced inside a crystal, when an incident X-ray plane wave satisfies or nearly satisfies the Bragg condition for a particular set of lattice planes. The energy flow of a wave field may propagate in any direction between the incident and the diffracted beam directions depending on the deviation from the exact Bragg condition*. However, the incident beam must generally be considered as a spherical wave, which is sufficiently divergent to cover the whole range of Bragg reflection. A fan of energy-flow directions, called the Borrmann delta, will then be set up simultaneously in the crystal.

The absorption of the wave fields is a function of the energy-flow direction. There will be high intensities at the edges of the Borrmann delta, as long as the average absorption is small. In the high-absorption case the edge intensity will be completely absorbed. The effective angular width of the Borrmann delta contributing to the diffracted intensity at the exit surface is reduced to $\Delta\alpha < 2\theta$, where α is the angle between a particular energy-flow direction and the lattice planes, and θ is the Bragg angle.

The intensity distribution within the Borrmann delta has been extensively studied for calcite¹⁻³ and silicon⁴. The divergence of the energy flow is of vital importance for the contrast in dislocation

images⁵ and for the spatial coherence width in interferometry^{3, 4, 6}.

It has been shown by the author⁷ that the intensity distribution within the Borrmann delta can be studied by shadow sharpness measurements. The shadow is produced by an absorbing wire placed close to the X-ray entrance surface of the crystal. Intensity profiles have been observed in the low-absorption as well as the high-absorption case in silicon single crystals.

In this work the Borrmann delta in germanium has been studied. All observations have been made in the high-absorption case due to the strong absorption in germanium. On the other hand, germanium offers the interesting possibility of studying the energy flow on both sides of an absorption edge. The K absorption edge of germanium is situated at 1.117 Å. Several suitable characteristic lines in the wavelength range from 1.541 Å to 0.709 Å have been obtained from copper, tungsten, gold, platinum and molybdenum targets.

2. Experimental

A slice of a dislocation-free germanium single crystal was cut parallel to the (111) planes. The thickness of the slice is 0.315 mm after mechanical and chemical polishing.

X-ray diffraction topographs were taken using Lang's traverse technique⁸ and the symmetric $2\bar{2}0$ reflection. Shadow images were produced by a platinum wire placed close to the X-ray entrance surface of the slice (Figure 1). The thickness of the wire is 0.35 mm.

Reprint requests to Dr. L. Gerward, Laboratory of Applied Physics III, Building 307, Technical University of Denmark, DK-2800 Lyngby, Denmark.

* The Laue case of diffraction is considered in this work.



Dieses Werk wurde im Jahr 2013 vom Verlag Zeitschrift für Naturforschung in Zusammenarbeit mit der Max-Planck-Gesellschaft zur Förderung der Wissenschaften e.V. digitalisiert und unter folgender Lizenz veröffentlicht: Creative Commons Namensnennung-Keine Bearbeitung 3.0 Deutschland Lizenz.

Zum 01.01.2015 ist eine Anpassung der Lizenzbedingungen (Entfall der Creative Commons Lizenzbedingung „Keine Bearbeitung“) beabsichtigt, um eine Nachnutzung auch im Rahmen zukünftiger wissenschaftlicher Nutzungsformen zu ermöglichen.

This work has been digitalized and published in 2013 by Verlag Zeitschrift für Naturforschung in cooperation with the Max Planck Society for the Advancement of Science under a Creative Commons Attribution-NoDerivs 3.0 Germany License.

On 01.01.2015 it is planned to change the License Conditions (the removal of the Creative Commons License condition "no derivative works"). This is to allow reuse in the area of future scientific usage.

Characteristic X-radiation was obtained from copper, tungsten and molybdenum targets in conventional fine-focus tubes. Gold and platinum targets were constructed and used in a micro-focus X-ray generator.

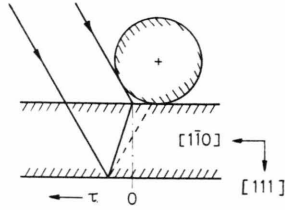


Fig. 1. Energy-flow directions pointing towards a point on the X-ray exit surface. An absorbing wire is placed close to the X-ray entrance surface.

The topographs were recorded on Ilford G5 plates. Microphotometer traces were taken perpendicular to the wire axis. The best precision was obtained by operating the microphotometer manually and measuring the optical density in discrete steps.

3. Theory

There will be four X-ray wavefields propagating in each direction α within the Borrmann delta. Their contribution to the diffracted intensity at the exit surface is given by⁹

$$I_h(p) = \sum_i C_i A (1 - p^2)^{-\frac{1}{2}} \cdot \cosh[C_i \mu t \varepsilon (1 - p^2)^{\frac{1}{2}}] \exp\{-\mu t\},$$

$$i = \sigma, \pi. \quad (1)$$

Here $C_\sigma = 1$ and $C_\pi = |\cos 2\theta|$ are the polarization factors, $A = \text{constant}$ related to the incident beam and diffraction conditions, $p = \tan \alpha / \tan \theta$, $t = t_0 / \cos \theta$, where $t_0 = \text{crystal thickness}$, $\mu = \text{linear absorption coefficient}$, $\varepsilon = F_h'' / F_0''$, the ratio of the imaginary parts of the structure factors F_h and F_0 respectively.

The following assumptions have been made: The incident beam is unpolarized and has a constant intensity within the angular range of Bragg reflection. The diffracting lattice planes are perpendicular to the surface of the crystal. The crystal structure is centrosymmetric with origin of coordinates at a symmetry centre. "Pendellösung" interference is neglected.

Each point on the exit surface diffracts an integrated intensity, when the crystal moves past the incident beam. The Borrmann delta is partly cut off

close to the absorbing wire (Fig. 1), so that the integrated intensity is given by

$$I_i(\tau) = \begin{cases} \int_{-1}^1 I_h(p') dp' = \bar{I}_i & \text{for } \tau > t_0 \tan \theta, \\ \int_{-1}^p I_h(p') dp' & \text{for } |\tau| \leq t_0 \tan \theta, \\ 0 & \text{for } \tau < -t_0 \tan \theta, \end{cases} \quad (2)$$

where τ is a coordinate along the exit surface and $p = \tau / (t_0 \tan \theta)$.

The intensity distribution (1) is centered around $p = 0$ in the high-absorption case, i. e. when $\mu t \gg 1$. It can be shown⁷ that the intensity profile (2) is linear for $p \ll 1$ and that the slope is given by

$$[d(I_i/\bar{I}_i)/dp]_{p=0} = [\mu t \varepsilon / (2\pi)]^{\frac{1}{2}}. \quad (3)$$

An effective width of the Borrmann delta is defined by extrapolating this linear region to I_i/\bar{I}_i equal to zero and unity respectively:

$$p_{\text{eff}} = (2\mu t \varepsilon / \pi)^{-\frac{1}{2}}. \quad (4)$$

The angular width is then given by

$$\Delta\alpha = 2 \arctan(p_{\text{eff}} \tan \theta). \quad (5)$$

4. Results and Discussion

Some examples of intensity profiles are shown in a normalized scale in Figures 2 and 3. The theoretical curves have been computed from (1) and (2) by numerical integration. The values of the absorp-

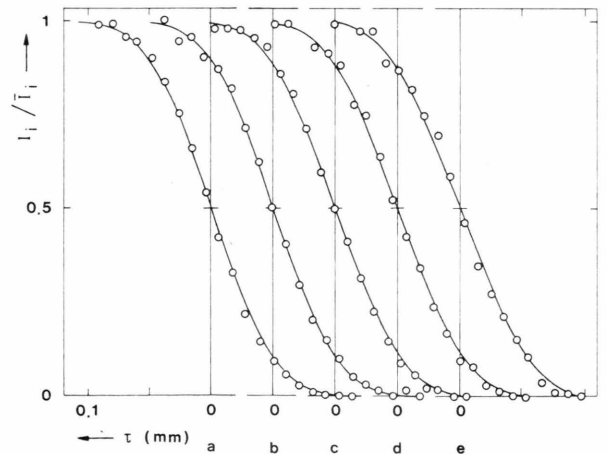


Fig. 2. Intensity profiles for photon energies below the K absorption edge of germanium. $2\bar{2}0$ reflection. Circles denote experimental values and full lines theoretical curves. (a) Cu $K\alpha_1$ radiation. (b) W $L\alpha_1$ radiation. (c) Pt $L\alpha_1$ radiation. (d) Au $L\alpha_1$ radiation. (e) Pt $L\beta_1$ radiation. The curves are displaced 0.05 mm on the τ scale from each other.

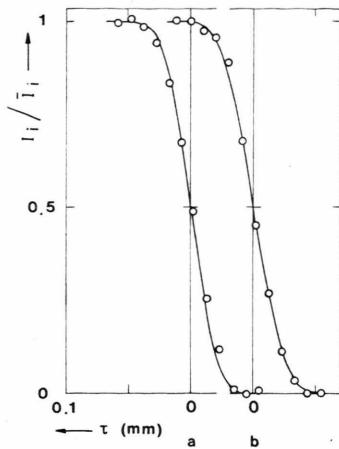


Fig. 3. Intensity profiles for photon energies above the K absorption edge of germanium. 220 reflection. Circles denote experimental values and full lines theoretical curves. (a) Au $L\beta_1$ radiation. (b) Mo $K\alpha_1$ radiation. The curves are displaced 0.05 mm on the τ scale from each other.

tion coefficient have been taken from measurements by Grimvall and Persson¹⁰. The values of ϵ have been taken from calculations by Persson and Efimov¹¹ based on Wagenfeld's¹² theory. The experimental and the theoretical intensity profiles have been fitted at the half maximum value.

More detailed results are given in Table 1. The experimental values have been obtained by extrapolating the linear central regions of the intensity profiles. Each experimental value quoted in Table 1 is the mean value of at least six photometric measurements at different positions on the plate. The error is the maximum deviation from the mean value.

It follows from Figs. 2 and 3 and Table 1 that the intensity profiles are very well described by (1) and (2). The observed widths of the Borrmann delta are in most cases slightly larger than the cal-

culated ones. This is most pronounced for the smallest widths. Systematic errors are introduced by the slit width of the photometer, total reflection of the incident X-rays at the surface of the wire, and the cylindrical shape of the absorbing wire. The maximum systematic error in the determination of Δa is estimated to 1.5° . When this error is taken into account there is a good agreement between the observed and calculated widths.

It is also seen in Figs. 2 and 3 and Table 1 that the shape of the intensity profiles and the angular widths are almost constant, regardless of the X-ray wavelength, on each side of the edge. The width is reduced drastically on the high-energy side of the absorption edge as compared with the low-energy side. These results can be explained by the expression (5) for Δa . A good approximation of the wavelength dependence of the absorption coefficient is

$$\mu = C \lambda^n, \quad (6)$$

where λ is the wavelength, and C and n are constants. The wavelength can be eliminated using Bragg's law and one obtains

$$\tan(\Delta a/2) = (2^{n+1} C d^n t_0/\pi)^{-1/2} g(\theta), \quad (7)$$

where d is the spacing of the Bragg planes and $g(\theta)$ is a slowly varying function of the Bragg angle. In the wavelength range used here $g(\theta)$ has the value 1.6 for Cu $K\alpha_1$ radiation, 1.8 at the K absorption edge of germanium, and 2.1 for Mo $K\alpha_1$ radiation.

It follows from (7) that the angular width is essentially a function of the crystal thickness for a given set of lattice planes. However, the value of C changes discontinuously at an absorption edge. Grimvall and Persson¹⁰ have found $C=103$ and $n=2.85$ [μ in cm^{-1} and λ in \AA in (6)] for the absorption due to the L - and M -electrons, and $C=749$ and $n=2.84$ for the absorption due to the

Table 1. Effective width of the Borrmann delta in germanium. 220 reflection, symmetric Laue case, $t_0=0.315$ mm. K absorption edge $\lambda_K=1.117$ \AA .

Line	$\lambda(\text{\AA})$	μt	p_{eff}	Experimental $\Delta a(^{\circ})$	Theoretical p_{eff}	Theoretical $\Delta a(^{\circ})$
Cu $K\alpha_1$	1.541	12.01	0.38 ± 0.01	18.0 ± 0.8	0.369	17.5
W $L\alpha_1$	1.476	10.47	0.42 ± 0.03	18.8 ± 1.2	0.395	17.8
Pt $L\alpha_1$	1.313	7.44	0.48 ± 0.04	18.9 ± 1.4	0.469	18.5
Au $L\alpha_1$	1.277	6.91	0.51 ± 0.04	19.6 ± 1.6	0.436	18.6
Pt $L\beta_1$	1.120	4.82	0.56 ± 0.03	18.8 ± 1.0	0.582	19.3
Au $L\beta_1$	1.084	34.92	0.27 ± 0.02	8.6 ± 0.6	0.216	7.0
Mo $K\alpha_1$	0.709	10.18	0.45 ± 0.05	9.4 ± 1.0	0.400	8.2

K-electrons. Inserting these values in (7) * shows that $\tan(\Delta\alpha/2)$ is reduced by a factor of about 2.9

when passing the absorption edge from the low-energy side to the high-energy side.

* The small difference in the value of the exponent n has been neglected for simplicity.

¹ G. Borrmann, *Naturwiss.* **42**, 67 [1955].

² G. Borrmann and H. Wagner, *Naturwiss.* **42**, 68 [1955].

³ G. Borrmann, G. Hildebrandt, and H. Wagner, *Z. Physik* **142**, 406 [1955].

⁴ K. Lehmann and G. Borrmann, *Z. Kristallogr.* **125**, 1 [1967].

⁵ G. Borrmann, W. Hartwig, and H. Irmeler, *Z. Naturforsch.* **13a**, 423 [1958].

⁶ U. Bonse and M. Hart, *Z. Physik* **188**, 154 [1965].

⁷ L. Gerward, *Physica Scripta* **4**, 71 [1971].

⁸ A. R. Lang, *Acta Cryst.* **12**, 249 [1959].

⁹ N. Kato, *Acta Cryst.* **13**, 349 [1960].

¹⁰ G. Grimvall and E. Persson, *Acta Cryst. A* **25**, 417 [1969].

¹¹ E. Persson and O. N. Efimov, *Phys. Stat. Sol. (a)* **2**, 757 [1970].

¹² H. Wagenfeld, *Phys. Rev.* **144**, 216 [1966].

The Borrmann Effect in Few-beam Electron Diffraction Patterns:

Use of the Born Series to Analyse Diffraction Asymmetries

P. Goodman

Division of Chemical Physics, CSIRO, Clayton, Victoria, Australia

(*Z. Naturforsch.* **28a**, 580–587 [1973]; received 1 February 1973)

Dedicated to Professor G. Borrmann on the occasion of his 65th birthday

A description is given of the Borrmann effect associated with a 3- and 4-beam interaction, as observed in the zero beam distribution of a Kossel-Möllenstedt electron diffraction pattern. In the 3-beam interaction which is studied in detail, the contribution to the intensity asymmetry is characterised by the order of the Born process. Considering the inversion symmetry about the central intersection, even order terms contribute an absorption effect, independent of the phase of the structure amplitude, while odd order terms contribute a structure dependent term which to the first order is independent of absorption. Considering the asymmetry across the weak line and parallel to the strong line, the absorption contributes an asymmetry which inverts with the sign of the structure amplitude. This latter property of the Borrmann effect has possible applications in structure analysis.

1. Introduction

The presence of a Borrmann¹ Effect in electron diffraction was recognized at least as early as Honjo and Mihama's (1954) report on fine structure patterns from MgO². Also many Kossel-Möllenstedt patterns showing asymmetries and other effects due to dynamic interactions with absorption were published, for example by Hoerni³. Since that time the complete n -beam dynamic theory has become available, so that the possible scope of an investigation is now very wide.

Quantitative examination of the Borrmann effect in electron diffraction can be made only by a detailed calculation of dynamic intensities, and for this purpose a fairly thorough knowledge of the structure is required. However, the recent renewed

interest in electron diffraction of structurally-unknown compounds indicates that there may be also room for more analytical approaches to dynamic scattering. Qualitative analysis of the Borrmann effect in Kossel-Möllenstedt patterns, i.e., of zero-beam asymmetries, can be rewarding in tracing the origins of asymmetry, in studies of structure and absorption. Few-beam patterns discussed here can be obtained by choice of orientation from crystals of moderate unit-cell size and moderate thickness, but must be interpreted through the complete theory to obtain reliable conclusions.

2. Theory

In 1957 an analytical solution to the n -beam scattering problem for forward scattering from a crystal of finite thickness became available⁴. This was later given as a Born series of products⁵,

$$U(h) = \sum_n E_n(h) \cdot Z_n(h) \quad (1)$$

Reprint requests to The Chief, Division of Chemical Physics, CSIRO, P.O. Box 160, Clayton, Victoria, Australien 3168.